

7-12-2020

Control Charts for Monitoring the Reliability of Multi-State Systems.

K. Genada

Production and Mechanical Design Engineering Department, Faculty of Engineering, Mansoura University, Egypt

M. Hussein

Production and Mechanical Design Engineering Department, Faculty of Engineering, Mansoura University, Egypt

A. Abdel-Shafi

Production and Mechanical Design Engineering Department, Faculty of Engineering, Mansoura University, Egypt

Follow this and additional works at: <https://mej.researchcommons.org/home>

Recommended Citation

Genada, K.; Hussein, M.; and Abdel-Shafi, A. (2020) "Control Charts for Monitoring the Reliability of Multi-State Systems.," *Mansoura Engineering Journal*: Vol. 40 : Iss. 4 , Article 14.

Available at: <https://doi.org/10.21608/bfemu.2020.102395>

This Original Study is brought to you for free and open access by Mansoura Engineering Journal. It has been accepted for inclusion in Mansoura Engineering Journal by an authorized editor of Mansoura Engineering Journal. For more information, please contact mej@mans.edu.eg.

Control Charts for Monitoring the Reliability of Multi-State Systems

خرائط تحكم لمراقبة معولية الأنظمة متعددة الحالات

K. Genada, M.-S. Hussein and A. A. Abdel-Shafi

Production and Mechanical Design Engineering Department, Faculty of Engineering, Mansoura University, Egypt

المخلص

كثيرا ما تستخدم خرائط التحكم كأدوات لمراقبة سلوك العمليات. ولكن في حالة العمليات ذات الجودة العالية، فإن استخدام خرائط تحكم شيورات التقليدية يكون غير ملائم. ولذا فقد تم إنشاء عدة أنواع من خرائط التحكم من أجل مراقبة حالة العمليات ذات الجودة العالية بناءً على التوزيع الأسّي وتوزيع واييل. ومن ثم تم تطوير هذه الخرائط لاستخدامها في رقابة المعولية. إن هذه الخرائط حتى الآن مخصصة لمراقبة معولية الأنظمة ثنائية الحالة والتي تمتلك فقط مستويين من الأداء: عاملة أو متوقفة. على الناحية الأخرى، فإن الأنظمة متعددة الحالات تمتلك مستويات مختلفة من الأداء. هذه الورقة البحثية تقدم نوعين جديدين من خرائط التحكم من أجل مراقبة معولية الأنظمة متعددة الحالات. كلا النوعين قادران على مراقبة انتقال حالات بمعدلات مختلفة باستخدام حدود التحكم ذاتها. النوع الأول هو خرائط التحكم ذات الحدود الزاوية. هذا النوع يصور حالات المنظومة على حدة ولكن بحدود التحكم ذاتها. من أجل هذا يستخدم هذا النوع من خرائط التحكم حدود تحكم احتمالية ذات زوايا ميل مختلفة. النوع الثاني هو خرائط التحكم التوزيع الأسّي المحول. هذا النوع يستخدم صورة محولة من التوزيع الأسّي كنموذج للزمن حتى حدوث العطل.

Abstract

Control charts are widely used tools for monitoring process behavior. However, for high-quality processes, using traditional Shewhart control charts is not appropriate. Thus, several types of control charts have been established for monitoring high-quality processes based on the Exponential and Weibull distributions. These charts were later adopted for reliability monitoring. So far, these charts have been dedicated for monitoring the reliability of binary-state systems, which have only two levels of performance—functioning or failed. On the other hand, multi-state systems exhibit different levels of performance. This paper introduces two new types of control charts for monitoring the reliability of multi-state systems. Both types monitor can monitor different state transitions with different rates using the same control limits. The first type is the Angular Limits Control (ALC) chart. The ALC chart depicts different system-state distinctively but with the same probability control limits. To achieve this, the chart uses probability control limits with different angles of inclination. The second type is the Transformed Exponential Control (TEC) chart. The TEC chart uses a transformed form of the Exponential distribution as a model for the time to fail.

Keywords

Reliability monitoring; Control charts; t_r -charts; Multi-state system reliability; Exponential distribution.

Abbreviations and nomenclature

ALC:	: Angular Limits Control	λ	: Failure rate
CDF:	: Cumulative Distribution Function	t	: Time to fail
CQC	: Cumulative Quantity Control	c	: False alarm probability
CUMSUM	: Cumulative Sum	θ_U	: Upper control limit angle
EWMA	: Exponentially Weighted Moving Average	θ_C	: Central line angle
MTTF:	: Mean Time to Failure	θ_L	: Lower control limit angle
PDF	: Probability Distribution Function	CCL	: Central Control Limit
TEC:	: Transformed Exponential Control	LCL	: Lower Control Limit
SS:	: System State	UCL	: Upper Control Limit

1. Introduction

1.1. Reliability Monitoring

Statistical process control charts are widely used tools for monitoring process behavior. However, for high-quality processes, where defect rate is low, traditional Shewhart control charts cease to be adequate. They encounter several problems, such as: high probability of generating false alarms, inability to detect change in process characteristics, unnecessary plotting of many zero points, meaningless upper and lower control limits, etc. That is because the frequency distribution of the occurrence of defects in high-quality processes is heavily skewed and cannot be adequately approximated to the normal distribution [1, 2].

To overcome these inadequacies, Chan et al. (2000) (cited in [3]) introduced the CQC- (Cumulative Quantity Control) and CQC_r -charts to monitor high-quality processes. The CQC-chart observes a certain quantity (e.g. time) between the occurrences of two events (e.g. defects), and uses probability limits instead of the traditional three-sigma limits. Similarly, CQC_r -charts observe a quantity between the occurrences of r events. In high-quality processes, the occurrence of a defect is commonly modeled as a homogenous Poisson process. Thus, the time observed between the occurrence of two defects follows an Exponential distribution [4].

Based on the CQC- and CQC_r -charts, Xie et al. [5] proposed the use of t - and t_r -charts for monitoring reliability. The t_r -charts monitors the time until r failures are observed. The Exponential, two-parameter Weibull, and Erlang distributions were used to model the time to fail in the t - and t_r -charts. However, any statistical distribution for positive variables can be used as a model for the time fail [2].

Other chart types were used to monitor the time between the occurrence of events, most common of them are the Exponential EWMA (Exponentially Weighted Moving Average) chart and the

Exponential CUMSUM (Cumulative Sum) chart [1, 3].

CQC- and CQC_r -charts are simple in design and easy to employ. They are more effective than Exponential EWMA and Exponential CUMSUM charts when process shifts are large and/or unpredictable. However, Exponential EWMA and Exponential CUMSUM charts outperform CQC- and CQC_r -charts in case of small and moderate process shifts, and/or when these shifts can be accurately predicted [3, 4, 6].

1.2. Multi-State Systems Reliability

Traditional reliability theory deals with systems in a binary way—functioning or failed. However, for many applications this classification is oversimplified and not sufficient. Many systems exhibit several levels of efficiency ranging from perfect functioning to complete failure. These varying levels of efficiency are called ‘performance rates’ or ‘system states’. A system that can have a finite number of performance rates/system states is called a multi-state system [7, 8].

Since the introduction of multi-state reliability theory in the 1970s, numerous research studies have been devoted to the subject. Fields of research in multi-state reliability include: reliability assessment and evaluation, reliability optimization, and maintenance planning [9]. However, using control charts for monitoring the reliability of multi-state systems has not been addressed in literature.

2. Control Charts for Multi-State Systems

The main problem with monitoring the time to fail for multi-state systems is that the system could have different failure rates corresponding to different states. This paper introduces two new types of control charts for monitoring the reliability of multi-state systems. Both charts monitor exponentially distributed time to fail; using the same control limits for different system states. These charts are based on the t -charts

established by Xie et al. [5]. The probability control limits are calculated from the inverse cumulative distribution function (CDF) of the Exponential distribution.

$$F_T^{-1}(p) = \frac{-\ln(1-p)}{\lambda} \quad (1)$$

3. Angular Limits Control Chart

The Angular Limits Control (ALC) chart uses control limits with different angles of inclinations. In order to give a good overall view of the system's behavior, this control chart depicts each system state (SS) distinctively.

In the ALC chart, the observed time to fail is measured on the horizontal axis. The vertical axis represents the mean time to fail (MTTF). Each SS is represented by a horizontal line crossing the vertical axis at the SS's MTTF.

Each observation point is depicted by a ray irradiating from the origin point. The end point of the ray rests on the line representing the observation's SS; and the projected horizontal distance represents the observed time to fail, t . Then, angle of inclination (see Figure 1) of any observation ray is

$$\theta = \text{atan}\left(\frac{\text{MTTF}}{t}\right) = \text{atan}\left(\frac{1}{\lambda t}\right) \quad (2)$$

3.1. Control Limits of ALC chart

The angle of inclination equation (Equation 2) can be applied to the probability control limits of the Exponential distribution (Equation 1) in order to determine the angles of inclination for the upper, central, and lower control limits— θ_U , θ_C , and θ_L , respectively. The false alarm probability, c , represents the acceptable probability of misdetection. The control limits' angles of inclination are

$$\theta_U = \text{atan}\left(\frac{1}{\lambda \times F^{-1}\left(1-\frac{c}{2}\right)}\right) = \text{atan}\left(\frac{-1}{\ln\left(\frac{c}{2}\right)}\right) \quad (3)$$

$$\theta_C = \text{atan}\left(\frac{1}{\lambda \times F^{-1}\left(\frac{1}{2}\right)}\right) = \text{atan}\left(\frac{-1}{\ln(2)}\right) = 55^\circ 16' \quad (4)$$

$$\theta_L = \text{atan}\left(\frac{1}{\lambda \times F^{-1}\left(\frac{c}{2}\right)}\right) = \text{atan}\left(\frac{-1}{\ln\left(1-\frac{c}{2}\right)}\right) \quad (5)$$

Equations 3-5 show that the control limits' angles of inclination do not depend on any of the failure rates. They depend only on the value of the false alarm probability, which is traditionally set to be 0.27%. Thus, a mulita-state system with differing failure rates will have the same control limits.

3.2. An Illustrative Example

The procedure of using the ALC chart will be illustrated using an example. Table 1 shows simulated times to fail, t , for 60 observation points for a multi-state system with three states (other than the perfect-functioning state): SS1, SS2, and SS3. The first 30 points is simulated, based on the Exponential distribution, with MTTFs of 1500, 3000, and 6000 hour, respectively. To depict process shifts, the next 30 points are simulated with the MTTFs of both SS1 and SS2 changed to 3000 hour.

The value false alarm probability is used as $c = 0.0027$, corresponding with the traditional three-sigma range. Equations 3 and 4 are used to calculate the angles of inclination for the upper and lower probability control limits.

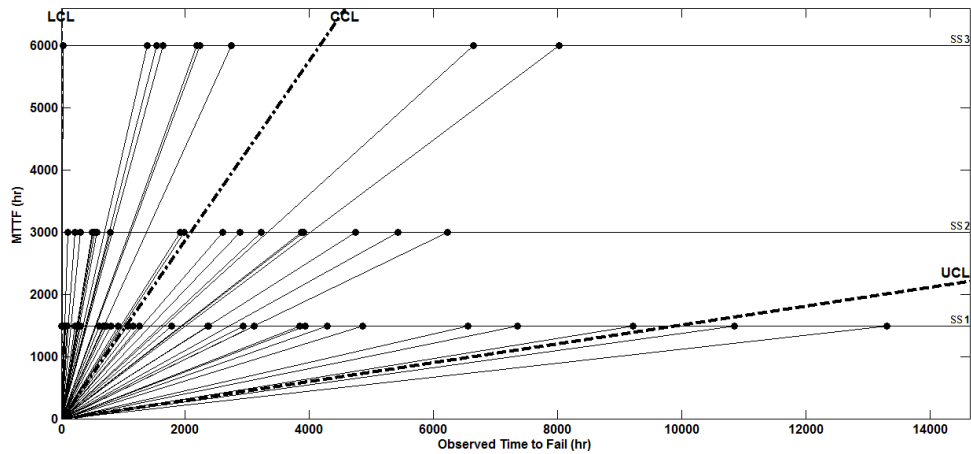
$$\theta_U = \text{atan}\left(\frac{-1}{\ln(1.35 \times 10^{-3})}\right) = 8^\circ 36'$$

$$\theta_L = \text{atan}\left(\frac{-1}{\ln(0.9987)}\right) = 89^\circ 55'$$

The data in Table 1 is plotted on an ALC chart in Figure 1. The chart detects out-of-control points in the case of SS1, which indicates an increase in the MTTF and possible improvement in this state. But it fails to detect the decrease in the MTTF for SS3.

Table 1. Time to fail for a multi-state system.

No.	SS	t (hr.)	No.	SS	t (hr.)	No.	SS	t (hr.)	No.	SS	t (hr.)
1	1	1255.7	16	1	2378.5	31	2	112.5	46	1	93.9
2	1	619.5	17	1	917.0	32	3	6639.5	47	3	1383.9
3	2	1976.1	18	3	26.9	33	2	516.2	48	1	684.2
4	1	1159.7	19	1	1781.7	34	3	2240.4	49	3	2742.9
5	1	66.2	20	1	682.5	35	1	6545.0	50	1	4285.5
6	3	8021.1	21	1	1070.2	36	1	801.0	51	2	3216.1
7	2	218.3	22	1	4854.7	37	2	5429.9	52	1	3930.4
8	1	9.0	23	1	729.1	38	2	3903.6	53	1	10845.4
9	2	1911.7	24	2	4736.8	39	2	304.0	54	1	7353.6
10	2	6226.4	25	2	3870.9	40	2	573.4	55	3	1532.2
11	1	311.4	26	1	2929.9	41	1	9210.3	56	2	794.3
12	1	219.1	27	1	48.6	42	2	494.9	57	3	1644.2
13	1	3843.6	28	1	1162.9	43	1	693.6	58	2	3900.5
14	1	2355.3	29	2	2602.6	44	1	3103.4	59	2	2885.3
15	2	538.1	30	1	262.9	45	3	2184.0	60	1	13303.2

**Fig. 1.** ALC chart for the data in Table 1.

3.3. Properties of the ALC Chart

In the ALC chart, an observation point with an angle of inclination θ less than θ_U , is an out-of-control point that represents a decrease in the failure rate; an indication of possible system improvement. Similarly, an observation point with angle of inclination θ greater than θ_L , is an out-of-control point that represents an increase in the failure rate; an indication of possible system deterioration.

Since the central control limit (CCL) represents the median of the data, then, if a system is in control, approximately 50% of the points will have angles of inclinations that are greater than θ_U , and the other 50% of the points will have angles of inclinations that are less than θ_U . This is true for the overall observation points, as well as the observation points for each system state separately.

The SS lines in the ALC chart are arranged ascendingly according to their MTTFs. And since events with higher failure rates will occur more frequently, lower SS lines should have more observation points than higher SS lines, if the system is in a state of control.

Figure 1 shows that the lower control limit nearly coincides with the vertical axis, which would make it difficult to detect points with $\theta > \theta_L$. To overcome this, the chart can be extended in the same manner as the t_r -charts to monitor the time

until r failures. In this case, the control limits' angles of inclination will be calculated using the Erlang distribution as a model for the time until r failures. This will also increase the overall sensitivity of the ALC chart.

The main drawback of the ALC chart is that it fails to clearly illustrate the timely sequence of failure events. As a solution, the sequence of each observation point could be written above it, as in Figure 2

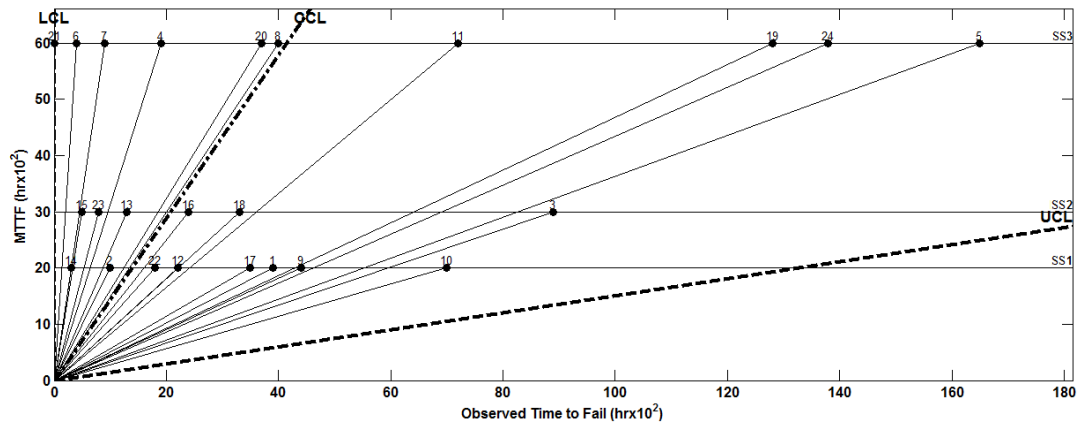


Fig. 2. ALC chart with numbered observations.

4. Transformed Exponential Control Chart

In the Transformed Exponential Control (TEC) chart, a transformed form of the Exponential distribution is used to model the time to fail. Using this transformed form of the Exponential distribution allows for modeling different state transitions with different failure rates using the same distribution. Thus, in the TEC chart different failure rates will have the same probability control limits.

4.1. Transformed Exponential Distribution

If a random variable T is exponentially distributed with a rate parameter of λ , then the probability distribution function (PDF) of T is

$$f_T(t) = \lambda e^{-\lambda t}, \quad t \geq 0 \quad (6)$$

Consider a dimensionless random variable, U , that is defined as the ratio between the observed time to fail, t , and the mean time to fail, MTTF. This random variable will be used to transform the PDF of the Exponential distribution. Based on the definition of the random variable U , the transformation and inverse transformation functions, respectively, are

$$u(t) = \frac{t}{MTBF} = \lambda t \quad (7)$$

$$t(u) = \frac{u}{\lambda} \quad (8)$$

Applying Equation 7 on the limits of the Exponential distribution ($0 \leq t \leq \infty$), gives the limits of the new distribution, which are also $0 \leq u \leq \infty$. The PDF of the new random variable U is derived from Equations 6-8 as

$$f_U(u) = f_T(t(u)) \frac{dt}{du} = \left(\lambda e^{-\lambda \frac{u}{\lambda}} \right) \times \left(\frac{1}{\lambda} \right) f_U(u) = e^{-u}, \quad u \geq 0 \quad (9)$$

Figure 3 show the PDF of the original Exponential distribution versus the PDF of the transformed exponential distribution for $\lambda = 0.5$ and 1.5 . If $\lambda = 1$, then the two PDFs will coincide with each other.

The PDF of the random variable U in Equation 9 is the transformed form of the Exponential distribution. For the random variable U , the CDF and inverse CDF, respectively, are

$$F_U(u) = \int_0^u e^{-x} dx$$

$$F_U(u) = 1 - e^{-u}, \quad u \geq 0 \quad (10)$$

$$F_U^{-1}(p) = -\ln(1 - p), \quad 0 \leq p \leq 1 \quad (11)$$

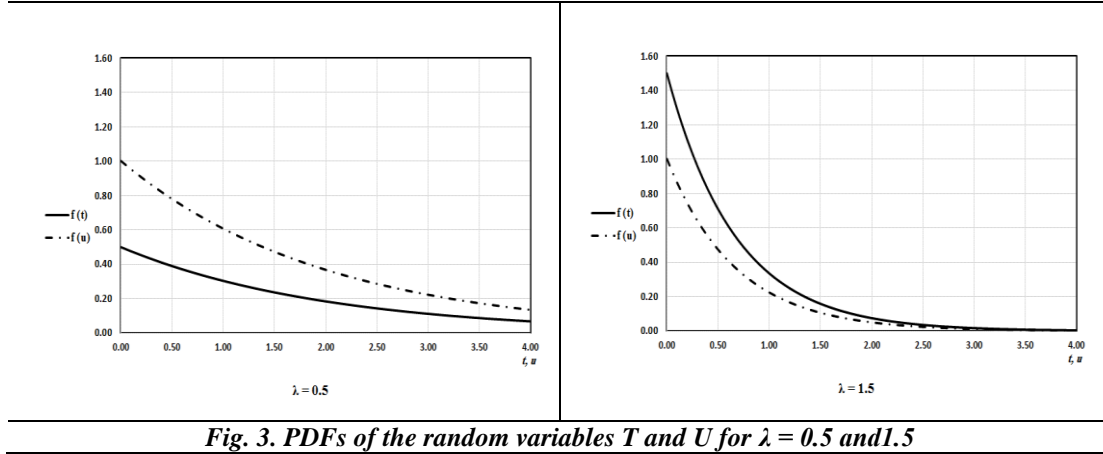


Fig. 3. PDFs of the random variables T and U for $\lambda = 0.5$ and 1.5

4.2. Control Limits of TEC chart

Based on the inverse CDF of the transformed Exponential distribution (Equation 11), the probability control limits of the TEC chart are

$$UCL = G^{-1}\left(1 - \frac{c}{2}\right) = -\ln\left(\frac{c}{2}\right) \quad (12)$$

$$CCL = G^{-1}\left(\frac{1}{2}\right) = -\ln\left(\frac{1}{2}\right) = 0.693 \quad (13)$$

$$LCL = G^{-1}\left(\frac{c}{2}\right) = -\ln\left(1 - \frac{c}{2}\right) \quad (14)$$

Equations 12-14 show that the values of the probability control limits depend only on the value of the false alarm probability, and not on any of the failure rates. To distinguish between different system-states, the state's number can be written above each observation point

4.3. An Illustrative Example

The data in Table 1 is used to illustrate the procedure of using the TEC chart. For a false alarm probability of $c = 0.0027$, Equations 12 and 14 are used to calculate values of the upper and lower probability control limits.

$$\theta_U = \text{atan}\left(\frac{-1}{\ln(1.35 \times 10^{-3})}\right) = 89^{\circ}36'$$

$$\theta_L = \text{atan}\left(\frac{-1}{\ln(0.9987)}\right) = 89^{\circ}55'$$

The data in Table 1 are plotted on a TEC chart in Figure 5. The chart detects the process shift in SS1 in the second part (the last 30 points) as most of the SS1 observation points are above the CCL line and are some are out-of-control (above UCL). This indicates an increase in the MTTF and possible system improvement. The process shift in SS3 can also be detected as nearly all the SS3 observation points in the second part (the last 30 points) are below the CCL line. This indicates a decrease in the MTTF and possible system deterioration

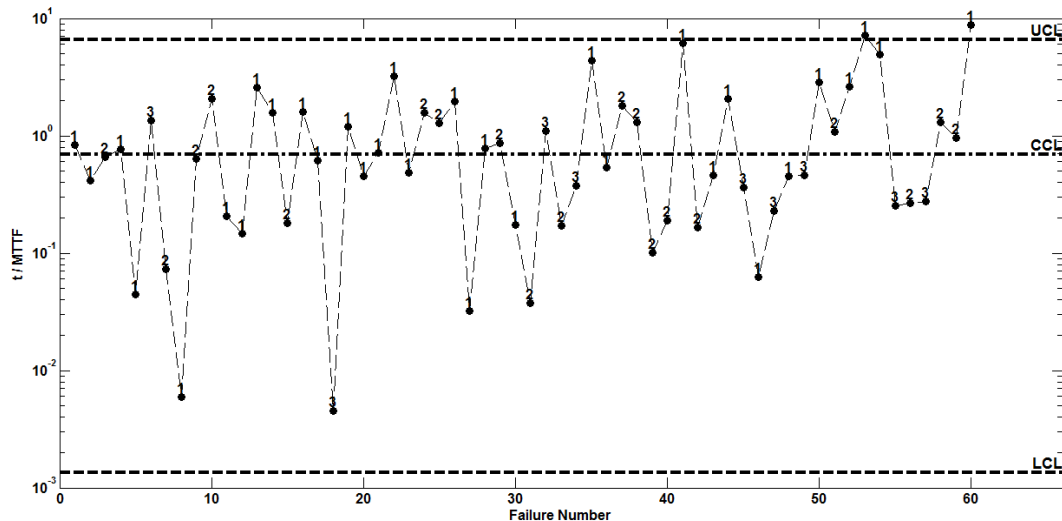


Fig. 4. TEC chart for the data in Table 1.

5. Conclusions

Several statistical control charts have been used to monitor the reliability of binary-state systems. For many applications, the binary view of systems is oversimplified and insufficient. This is why multi-state system reliability theory has been established. However, the subject of monitoring the reliability of such systems has not been addressed in literature.

This paper introduces two new types of control charts for monitoring the reliability of multi-state systems: the ALC chart and the TEC chart. These charts use the same control limits for different failure rates.

Angular control limits are used to establish the ALC chart. This chart is useful in giving a distinctive view of different system states' behaviors. A transformed Exponential distribution is used to establish the TEC chart. This form allows for modeling different state transitions with different failure using the same distribution. The TEC chart gives better results in detecting process shifts. This is due to the absence of the timely sequence of observations in the ALC chart. The two charts can be used jointly to give a better overall view of the system behavior.

Future work can be directed to adapting the ALC and TEC charts into other statistical distributions other than the Exponential (e.g. Weibull distribution). This will help to widen their range of applications. The ALC chart can be also extended in the same manner as the t_r -charts to monitor the time until r failures. This will increase the chart's ability and sensitivity for detecting system degradation.

Acknowledgment

This research paper is made possible through the help and support of Prof. Dr. Hassan Soltan, who initiated the idea of this work and followed up with constant encouragement. His guidance and insightful comments are much appreciated.

References

- [1.] Xie, M., Goh, T.N., Kuralmani, V.: Statistical Models and Control Charts for High-Quality Processes. Springer US, Boston, MA (2002).
- [2.] Pham, H. ed: Springer Handbook of Engineering Statistics. Springer London, London (2006).
- [3.] Liu, J.Y., Xie, M., Goh, T.N., Sharma, P.R.: A Comparative Study of Exponential Time between Events

- Charts. Qual. Technol. Quant. Manag. 3, 347–359 (2006).
- [4.] Yen, F.Y., Chong, K.M.B., Ha, L.M.: Synthetic-Type Control Charts for Time-Between-Events Monitoring. PLoS One. 8, (2013).
- [5.] Xie, M., Goh, T.N., Ranjan, P.: Some effective control chart procedures for reliability monitoring. Reliab. Eng. Syst. Saf. 77, 143–150 (2002).
- [6.] Fang, Y.Y., Khoo, M.B.C., Teh, S.Y., Xie, M.: Monitoring of Time-Between-Events with a Generalized Group Runs Control Chart. Qual. Reliab. Eng. Int. (2015).
- [7.] Lisnianski, A., Frenkel, I., Ding, Y.: Multi-state System Reliability Analysis and Optimization for Engineers and Industrial Managers. Springer London, London (2010).
- [8.] Levitin, G., Lisnianski, A.: A new approach to solving problems of multi-state system reliability optimization. Qual. Reliab. Eng. Int. 17, 93–104 (2001).
- [9.] Yingkui, G., Jing, L.: Multi-State System Reliability: A New and Systematic Review. Procedia Eng. 29, 531–536 (2012).